Soft Matter

Accepted Manuscript

ROYAL SOCIETY OF CHEMISTRY

www.rsc.org/softmatter

For Table of Contents Use Only

Disclosed New Evidence for Networking in Natural Rubber by Dielectric Relaxation Spectroscopy

Jie Liu, Siwu Wu, Zhenghai Tang, Tengfei Lin, Baochun Guo, and Guangsu Huang**

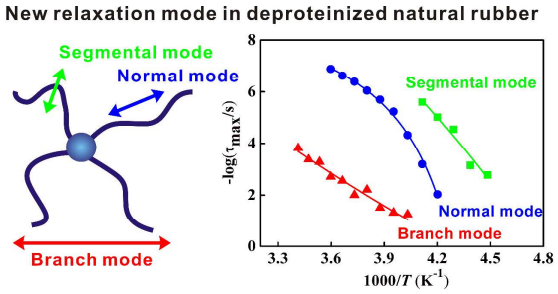

Branch relaxation mode is identified for the first time, which provides new implication for natural networking structure in natural rubber.

Disclosed New Evidence for Networking in Natural Rubber by Dielectric Relaxation Spectroscopy

Jie Liu,[a] Siwu Wu,[a] Zhenghai Tang,[a] Tengfei Lin,[a] Baochun Guo*[a] and Guangsu Huang*[b]

Received (in XXX, XXX) Xth XXXXXXXXX 20XX, Accepted Xth XXXXXXXXX 20XX
DOI: 10.1039/b000000x

Resolving the structure of natural rubber (NR) has been an important basic issue for a long time although essential progress has been made. It is well established that non-rubber components have significant effects on the performance of NR. The detailed discussion on the effect of proteins and phospholipids on the chain dynamics of NR will be fundamentally crucial to the in-depth understanding of the role of proteins and phospholipids in NR. However, there is still a lack of elaborate study on the dielectric spectroscopy of NR until now. In the present study, we performed detailed dielectric relaxation analysis, together with the rheological measurements, to reveal the effects of proteins and phospholipids on the chain dynamics of NR. Distinctly different from the widely accepted segmental mode (SM) and normal mode (NM), a new relaxation mode in deproteinized NR (DPNR) is identified for the first time, which can't be found either in NR or in transesterified DPNR (TE-DPNR). Since this new mode relaxation process behaves as a thermally activated process and it is about four orders of magnitude slower than NM, it could be rationally attributed to the relaxation of the phospholipids core of DPNR, named as branch mode (BM) relaxation. When further conversion of DPNR into TE-DPNR is conducted, the phospholipids are removed and BM disappears. In addition, a new relaxation mode which occurs at much lower temperature than that for SM is revealed in TE-DPNR, and it may be correlated to the relaxation of free mono- or di-phosphate groups at the α ends in TE-DPNR. Hence, the identification of the new relaxation modes in DPNR and TE-DPNR provide new evidence for the natural networking structure linked by protein-based ω ends and phospholipids-based α ends.

Introduction

Natural rubber (NR) from Hevea brasiliensis is widely applied for its excellent comprehensive properties, such as high tensile and tear strength, good crack growth resistance and minimal heat buildup compared to its synthetic counterpart polyisoprene (PI) which contains isoprene units with *cis*-1,4 configuration higher than 98% like NR chain.[1,2] Previous structural studies of NR by Tanaka revealed that NR comprises of two *trans*-isoprene units connected to a long-chain *cis*-isoprene units as well as two terminals.[1] It has been postulated that α-terminal links with mono- or di-phosphate groups which associate with phospholipids by H-bonding or ionic bonds, whereas the ω-terminal is a dimethylallyl group that links to proteins by H-bonding.[2,3] The presence of proteins and phospholipids in NR induces a multi-scaled microstructure formed by natural cross-linking among the terminal groups of linear polyisoprene chains.[4,5] The proposed structure of a linear rubber chain and naturally occurring networking in NR can be schematized in Fig. 1.[6,7]

It has been well-established that the outstanding properties of NR are closely related to the non-rubber components in NR, such as fatty acid (linked and mixed), proteins and phospholipids. Proteins presented in NR can be removed by deproteinization with proteolytic enzyme and surfactant,[1,8,9] and phospholipids can be decomposed by transesterification with sodium methoxide (CH_3ONa) to form linear rubber molecules.[1,10-12]

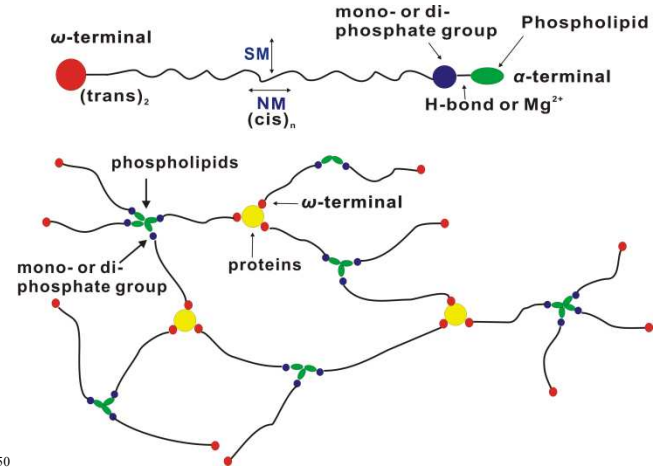

Fig.1 Proposed structure of NR networking.[6,7]

The effects of proteins and phospholipids on strain induced crystallization (SIC),[13] mechanical properties and gel formation of NR have been extensively studied by X-ray diffraction,[2,14,15] AFM and other methods.[16-19] Toki *et al*. studied stress-strain relation and SIC of natural rubber by synchrotron X-ray at various temperature from 223K to 308K and provided the schematic model of NR under undeformed and deformed state.[17,20] It's said that pseudo end-linked networking in NR makes entanglements as permanent entanglements, which can induce SIC and stress upturns during extension. Suchiva *et al*. reported that the tensile property of purified NR was deteriorated comparing to NR in both gum and carbon black-filled vulcanizate systems.[21,22] The roles of proteins and phospholipids in crack growth, abrasion resistance and dynamic properties in filled NR

and SBR/NR systems are also extensively studied.[23-27] Nor-Hidayaty *et al*. studied the curing behavior, crosslink density and dynamic load analysis of deproteined natural rubber (DPNR) vulcanisates.[28] Rattanasom *et al*. compared the abrasion loss and heat buildup properties of carbon black-filled DPNR vulcanizates to synthetic *cis*-1,4 polyisoprene vulcanizates at various crosslink densities and found that the heat buildup resistance of DPNR and IR at a given crosslink density was similar.[29] Santangelo *et al*. concluded that the fatigue resistance of guayule rubber and DPNR in the double networks was higher than their single network counterparts.[30] All of the research elaborated the importance of the proteins and phospholipids to the structure, property and applications of NR.

However, a detailed analysis on how proteins and phospholipids affect the chain dynamics of NR is still lacking. Dielectric spectroscopy is a sensitive tool for probing into the multi-level molecular units relaxation which contributes to a better understanding of the structure-property relationships. In order to better understand the mechanical and other properties on molecular unit concepts, one should probe into the molecular dynamics. NR consists basically of *cis*-1,4-PI chains with low-polarity. Due to the asymmetrical structure of *cis*-PI, NR has dipole moment both parallel and perpendicular to the chain contour.[31] Therefore, NR exhibits a segmental mode relaxation (SM) which is caused by the perpendicular component of the dipole as well as a normal mode relaxation (NM) due to the parallel component under external electric field, as depicted in Fig. 1.[32,33] Several literatures have reported the dynamics of PI by dielectric analysis[34-37] and a few others covered on natural rubber are also accomplished.[33,38-41] However, to the best of our knowledge, the chain dynamics of the DPNR and transesterified deproteinized natural rubber (TE-DPNR) are rarely reported. Carretero-Gonzalez *et al*. used dielectric spectroscopy to investigate the dynamics of cleaned natural rubber (CNR), DPNR, TE-DPNR and the gel fraction. They compared different dynamic relaxations and got the result that SM is not effected by naturally occurring network while NM seems to be strongly affected by natural chain-end cross-linking.[4] However, their method of sample preparation for dielectric measurement is to dissolve rubber into toluene solution and then cast solution using a dropper, which makes it impossible to accurately define the thicknesses of samples over the whole temperature range covered by the measurements, resulting in the difficulty in analyzing the dielectric data based on dielectric loss strength. Therefore, a more detailed and quantitative analysis on the chain dynamics of DPNE and TE-DPNR by dielectric spectroscopy is still lacking.

The detailed discussion on the effect of proteins and phospholipids on the chain dynamics of NR will be fundamentally crucial and valuable. In addition, in-depth understanding of the role of proteins and phospholipids in NR is a key issue to mimic the NR natural network, which has profound significance to solve the shortage of NR. In our study, we used flat dried rubber to get the exact thicknesses for each system to reveal the effects of proteins and phospholipids on the chain dynamics of NR in a more detailed and quantitative way.

Experimental

Materials

NR latex with a solid content of 60 wt% was kindly provided by China Hainan Rubber Industry Group Co., Ltd. Sodium dodecyl sulphate (SDS) was purchased from Tianjin Fuchen Chemical Reagents Factory. Alcalase 2.4L enzyme was obtained from Novozymes in Denmark. DPNR was prepared by incubation of NR latex with 1% w/v SDS used as a stabilizer and 0.15 parts of Alcalase 2.4L enzyme per one hundred parts of dried rubber for 48 h at 310K followed by centrifugation at 13000 rpm for 30 min.[31,42] The cream fraction was redispersed with distilled water and recentrifuged once more. This process removes the proteins essentially.[38,40] TE-DPNR was prepared in toluene solution by reacting DPNR with freshly prepared CH_3ONa at room temperature under stirring for 3 h, followed by precipitation in excess methanol.[1] This transesterification process liberates the phospholipids in DPNR.[9,10]

Characterization

The protein content was determined from the nitrogen content (%N) using the Kjeldahl method.[42] Briefly, the sample was digested in strong sulfuric acid solution with Kjelblet (K_2SO_4:$CuSO_4{\cdot}5H_2O$, 9:1) as the catalyst which converted the amine nitrogen to ammonium ions. The ammonium ions were then converted into ammonia gas by heating and distillation, and entrapped in an acid solution. Finally, the amount of the trapped ammonia that correlated to the nitrogen content was determined by titration with 0.1 N of sodium hydroxide. The protein content was calculated by multiplying the %N with a Kjeldahl factor of 6.25 as follows in Equation 1.

$$\% \text{ protein} = 6.25\ (\% \text{ N}) \quad (1)$$

Nitrogen content tests show that protein content decreases remarkably from 2.243% w/w for NR to 0.277% w/w for DPNR. These results ensure the effect of protein removal through deproteinization and centrifugation. After transesterification, the nitrogen content of TE-DPNR was reduced close to zero, which is consistent with the literatures.[12,43]

Tensile tests were performed on U-CAN UT-2060 following ISO 37-2005. The measurement was carried out at room temperature with the testing crosshead speed of 500 mm/min. The thickness of dumbbell shape samples was about 1 mm and the measurement was repeated for 5 times for each sample.

The strain sweep and frequency analysis of NR, DPNR and TE-DPNR were performed on a RPA 2000 Rubber Processing Analyzer (ALPHA, USA) on the temperature of 333K. The strain sweeping (0.28%-100%) was conducted at the frequency of 60 cpm and the frequency sweeping (2-2000 cpm) was conducted at strain of 0.5%.

Small-angle X-ray scattering (SAXS) measurements for dry NR and DPNR films were carried out on NanoSTAR instrument (Bruker-AXS, Germany) at room temperature. The wavelength of X-ray was 1.54 Å. The sample thickness is 1.06mm for NR and 1.04mm for DPNR.

Broadband dielectric relaxation spectra (BDS) was conducted over a broad frequency range (10^{-1} ~10^{7} Hz) and wide temperature range (123~373K). The temperature intervals were set as 5 K and 2 K for frequency sweeping and temperature sweeping (fixed frequency at 7 Hz), respectively. All the data was collected on an ALPHA-ANB Broadband dielectric/impedance spectrometer (Novocontrol Technologies GmbH, Hundsangen,

Cite this: DOI: 10.1039/c0xx00000x

www.rsc.org/xxxxxx

ARTICLE TYPE

Germany). The flat dried samples with a thickness of about 1 mm were placed between two parallel gold-plated electrodes 20 mm in diameter. The temperature in these experiments was controlled by a nitrogen jet, thus having a temperature error of 0.1K during every single frequency sweeping.

Results and Discussion

The tensile experiments were conducted first to examine the possible effects of deproteinization and transesterfication on the mechanical responses of NR (Fig. S1). The results indicate that NR including α and ω- terminals exhibits SIC phenomena at the strain of almost 400%. For DPNR which only includes α-terminal entanglement, SIC is still observed and break stress decreases slightly compared to NR. However, the tensile strength of TE-DPNR that consists of neither α- terminal nor ω-terminal deteriorates significantly and does not exhibit SIC any more, indicating the significant influence of natural networking on the mechanical properties, especially for α- terminal entanglement. Such observations are consistent with the results from other researchers.[12,18,44]

The strain sweeping and frequency sweeping were conducted to examine the dependence of rheology on the deproteinization and transesterification. The strain sweeping results are shown in Fig. 2(a) and Fig. 2(b), respectively. It can be seen from Fig. 2(a) that with increasing strain, the storage shear modulus of three samples are basically constant at low strain (<10%) and decrease significantly at larger strain. The decrease of G' at higher strain (>10%) may be related to the disentanglement of the long NR chains. Within the overall range of sweeping strain, the storage shear modulus of NR is always higher than those for DPNR and TE-DPNR. This may be due to the different degree of networking for them and these variances in degree of networking result in different network knots density. Fig. 2(b) indicates that the tangents of loss angles (tan δ) of all samples stay almost unchanged with the strain rising and the tan δ of TE-DPNR is a little higher than the other two. This result is expected considering the structural variations among them. With the α-terminal and ω- terminal crosslinking structure, it is difficult for NR to deform under strain and it shows higher storage shear modulus than DPNR, in which the ω- terminal crosslinks are destructed after the deproteinization. As both α- terminal and ω-terminal corsslinks are eliminated, it is easy for TE-DPNR to deform under strain, therefore the storage shear modulus of TE-DPNR with linear PI chain structure is the lowest and its tan δ is the highest.

Fig. 2(c) depicts the responses of storage shear modulus to oscillation frequencies. It is obvious that the storage modulus rises with the increased oscillation frequency and the sharp rising tendencies appear at lower frequency range (<200cpm) for all samples. TE-DPNR has significantly lowered storage modulus comparing to those of NR and DPNR at the whole temperature range. Furthermore, the tan δ of the three samples decrease sharply at lower frequency (<200 cpm), while maintain their value at the higher frequency range as shown in Fig. 2(d). Within the whole range of sweeping frequency, the tan δ of TE-DPNR is higher than those of NR and DPNR. This should be attributed to the decomposition of the proteins linked to ω- terminal and the phospholipids linked to α- terminal of NR chains after deproteinization and transesterification, which results in the destruction of networking in NR.

SAXS intensity functions $I_{saxs(s)}$ of NR and DPNR are shown in Fig. S2. The scattering intensity of NR indicates the presence of strong density fluctuations at low s but without any periodical order. After deproteinization, the upturn in $I_{saxs(s)}$ is much alleviated in DPNR. Hence, it can be concluded that the upturn in $I_{saxs(s)}$ of NR may be due to inhomogeneity inherent of NR. The inhomogeneity has been considered to be originated from the aggregates of non-rubber components.[45] As the main part of the non-rubber components, the proteins are removed essentially after deproteinization.

The above RPA and SAXS tests indicate that the networking and entanglements from proteins and phospholipids have great influence on the structure and properties of NR. In order to further elucidate the influence of network structure on NR dynamic movements at the molecular unit level, BDS of above samples is investigated.

Temperature dependences of dielectric spectroscopy were analysed first. Fig. 3 and Fig. S3 show the dependences of ε" and ε' as a function of temperature for NR, DPNR and TE-DPNR at the fixed frequency of 7Hz, respectively. Here, we focus on ε" data to reveal NR dynamic movements. As expected, all three samples exhibit a relaxation related to the dynamic glass transition of NR long chain,[34] which should be assigned to the SM relaxation of NR chains (indicated by black arrows). SM relaxation is a fluctuation occurring at a length scale of about 2 to 3 chain segments and not much affected on the networking density differences, therefore it is reasonable to find that there is no much difference in the SM relaxation temperature among these three systems.

A second relaxation peak which should be assigned to NM relaxation is detectable at 268K, 228K and 308K for NR, DPNR and TE-DPNR, respectively (as red arrows indicate). It is evident that the temperature position of the NM maximum in ε″ varies from each other. At the same time, there are significant differences in dielectric loss strength among them. The peak values of ε″ for NM in Fig. 3 are summarized in Table S1. It shows that NR has the largest NM peak value of ε″ and the NM peak value of TE-DPNR is the least. Since NM is actually the fluctuation of end-to-end vector of the chain, its dielectric loss intensity will reinforce as the chain polarity increases. NR includes proteins and phospholipids. DPNR includes only phospholipids while neither proteins nor phospholipids are included in TE-DPNR. Considering the fact that both proteins and phospholipids are polar components, these differences in peak values of ε″ in Fig. 3 are reasonable.

The isochrones are useful to identify the relaxation processes of the samples in a visual way, but the quantitative analysis has to be carried out in the frequency domain for a detailed analysis. Therefore, isothermal representations are necessary. Typical dielectric loss spectras of NR, DPNR and TE-DPNR as a function of frequency at the corresponding relaxation temperature are shown in Fig. 4. As one can see from Fig. 4(a), a clear loss peak which should be due to the SM relaxation emerges when the test temperature is up to 218K for NR (as the black arrow).[34] This SM relaxation peak shifts to higher frequency with increasing temperature, which is known as thermally activated process. DPNR experiences the same SM relaxation at 228K as the black arrow in Fig. 4(b). However, after careful inspecting on the spectra of Fig. 4(a) and 4(b), it's not difficult to find that the SM peak of DPNR at 228K (as the black arrow indicates in Fig. 4(b)) emerges at lower frequency than the peak of NR at the same temperature (as the red curve in Fig. 4(a)). In other words, SM relaxation of DPNR is slower than NR.

Fig. 4(c) depicts the spectra of TE-DPNR at the SM relaxation temperature range. Similar to NR and DPNR, all SM relaxation peaks for TE-DPNR shift to higher frequencies as the temperature increases, according with thermally activated process. In order to analyze the SM relaxation quantitatively, we fit the typical frequency spectra using the Havriliak-Negami function with a conductivity term.[46,47]

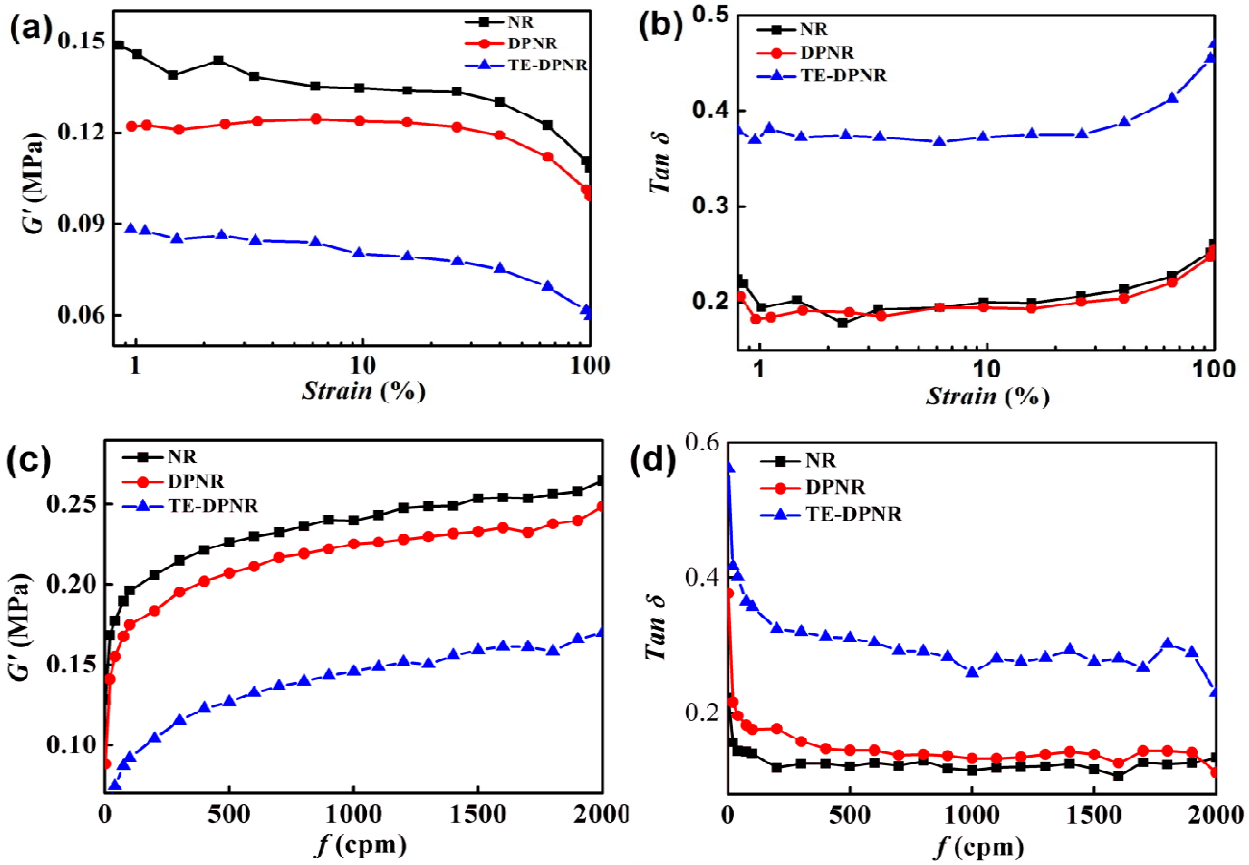

Fig.2 Responses of storage modulus and tan δ to strain (a and b) and frequeny (c and d)

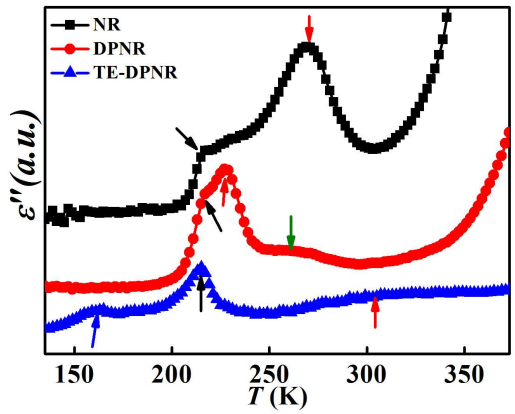

Fig.3 Temperature dependence of dielectric loss (ε″) at 7 Hz. The black, red, green and blue arrows indicate the peaks of SM, NM, branch mode and low temperature relaxation process, respectively. The spectras for NR and DPNR are shifted vertically for clarity.

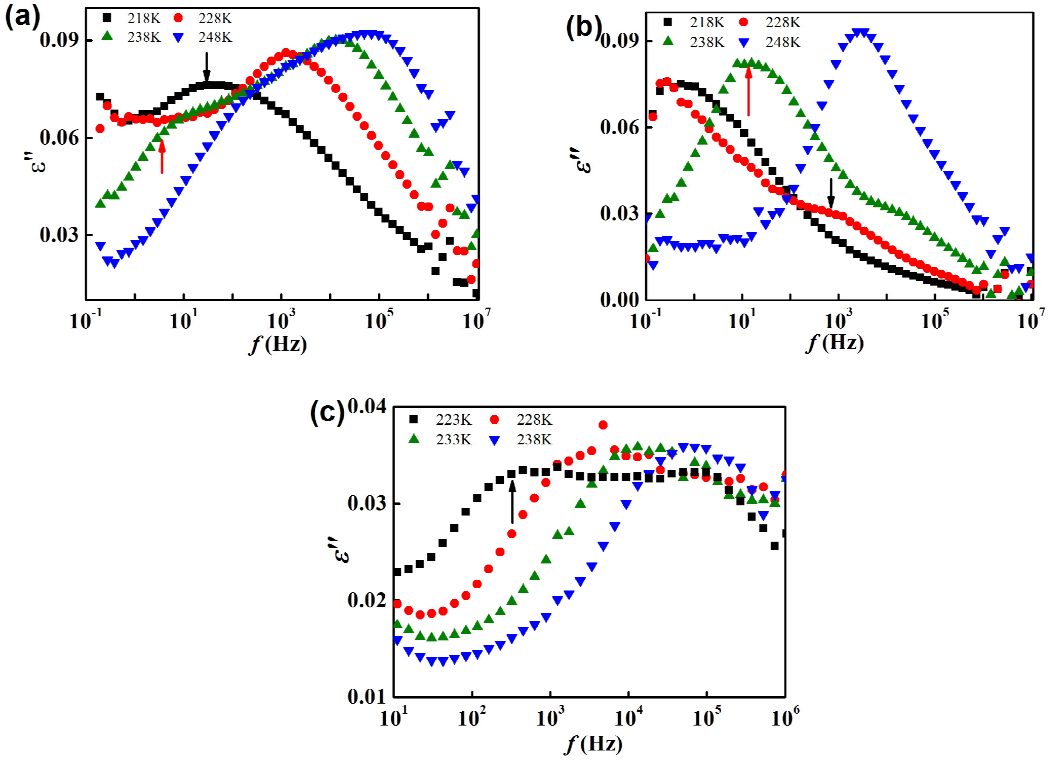

Fig.4 Dielectric loss ε″ vs. frequency of NR at 218K to 248K (a), DPNR at 218K to 248K (b), TE-DPNR at 223K to 238K (c). The black and red arrows indicate the emerging of SM and NM relaxation peaks, respectively.

The analysis was performed using Equation 2 that combines the conductivity term with the Havriliak-Negami functional form for each relaxation process, where $\omega = 2\pi f$, f is the frequency of the applied electric field, where ε_0 is the vacuum permittivity, σ_{dc} is the specific dc conductivity, N is an exponential factor ($0<N\leq1$), $\triangle\varepsilon_k=\varepsilon_{sk}-\varepsilon_\infty$ is the dielectric strength of the k_{th} process, ε_{sk} and ε_∞ are the unrelaxed and relaxed values of dielectric constant of the k_{th} process respectively, α_k and β_k are the shape parameters which describe the symmetric and asymmetric broadening of the k_{th} process, respectively ($\alpha_k>0$, $\beta_k\leq1$), and τ_{0K} is the Havriliak-Negami relaxation time representing the most approximate relaxation time of the maximum peak in ε''. The frequency of maximum loss is described by $f_{max} = 1/(2\pi\tau_{max})$. The relation between τ_0 and τ_{max} is given by Equation 3.[46,48]

$$\varepsilon^*(\omega)=\varepsilon'-i\varepsilon''=-i\left(\frac{\sigma_{dc}}{\varepsilon_0\omega}\right)^N+\sum_{k=1}^{n}\left[\varepsilon_{\infty k}+\frac{\Delta\varepsilon_k}{(1+(i\omega\tau_{0k})^{\alpha_k})^{\beta_k}}\right] \quad (2)$$

$$\tau_{\max} = \tau_0 [\frac{\sin\frac{\pi\alpha\beta}{2(1+\beta)}}{\sin\frac{\pi\alpha}{2(1+\beta)}}]^{1/\alpha}; \quad f_{\max} = \frac{1}{2\pi\tau_{\max}} \tag{3}$$

The real and imaginary parts of Equation 2 can be separated into:

$$\varepsilon'(\omega) = \varepsilon_\infty + \gamma^{-\beta/2}(\varepsilon_0 - \varepsilon_\infty)\cos\beta\theta \tag{4}$$

$$\varepsilon''(\omega) = \gamma^{-\beta/2}(\varepsilon_0 - \varepsilon_\infty)\sin\beta\theta \tag{5}$$

where

$$\gamma = [1 + (\omega\tau_0)^\alpha \sin(\frac{\alpha\pi}{2})]^2 + [(\omega\tau_0)^\alpha \cos(\frac{\alpha\pi}{2})]^2$$

$$\theta = \tan^{-1}[\frac{(\omega\tau_0)^\alpha \cos(\frac{\alpha\pi}{2})}{1 + (\omega\tau_0)^\alpha \sin(\frac{\alpha\pi}{2})}]$$

Typical fittings of the dielectric loss data of NR, DPNR and TE-DPNR at 223K using the HN function containing a conductivity term are shown in Fig. S4. Some of the SM fitting parameters in the illustrated spectra are summarized in Table S2.

In order to compare the different SM relaxation in a more direct fashion, all the segmental relaxation times obtained from HN fitting are transformed into τ_{max} by Equation 3. The temperature dependence of segmental relaxation time is well stated by Vogel-Fulcher-Tammann (VFT) equation (Equation 6), where τ_0 and B are temperature-independent constants, T_0 is the ideal glass transition temperature, B can be defined as $B=D \cdot T_0$, where D is referred to as the fragility strength parameter and is often used to quantify the extent by which the temperature dependence of the relaxation times deviates from Arrhenius behavior. τ_{max} for SM is plotted as a function of inverse temperature and depicted in Fig. 5.

$$\tau_{\max} = \tau_0 \exp(\frac{B}{T - T_0}) \tag{6}$$

When we discuss the SM relaxation of these three systems, we first consider NR as a networking structure as shown in Fig. 1. After deproteinization, the crosslinks in ω-terminal are eliminated and DPNR should be regarded as a star structure with the phospholipids as the star core and NR long chain as the arms. TE-DPNR, similar to linear PI, has no network structure.[2]

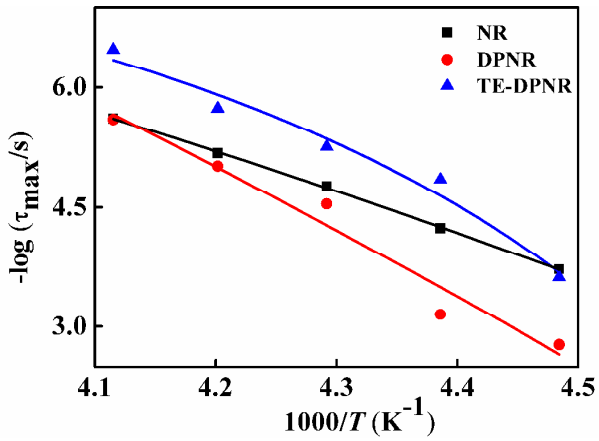

Fig.5 Activation plot for the segmental modes for NR, DPNR and TE-DPNR. The lines represent the fits of Equation 6.

As can be seen from Fig. 5, τ_{max} for TE-DPNR is much smaller than the other two at the same temperature, demonstrating its fastest SM process. In earlier report, Kramarenko *et al.* studied the effect of crosslinking on the segmental dynamics in model polymer networks and concluded that segmental motions above the glass transition experience a growing hindrance and shift towards higher temperatures as the cross-linking density increases.[49] Therefore, the fastest SM relaxation should be expected. When we compare the curves of NR and DPNR in Fig. 5, we can find that DPNR has slower SM relaxation than NR. This finding seems, at first glance, to be unreasonable as DPNR has lower crosslinking density than NR. However, we cannot ignore the fact that there is a little mixed fatty acid in NR latex and the mixed fatty acid can be removed during the process of centrifugation for the preparation of DPNR. This mixed fatty acid included in NR can act as plasticizer in this experiment, which promotes the movements of NR segment chain. Considering this factor, this result can be understandable.

Besides SM relaxation, all three samples exhibit NM relaxation at higher temperature as the red arrows indicate in Fig. 3. This NM relaxation appears as a consequence of the dipole moment parallel to the chain contour.[4] The frequency spectra of NM relaxation for NR, DPNR and TE-DPNR can be found in Fig. 4(a), Fig. 4(b) and Fig. 6(a) as the red arrows indicate.

Fig. S5 and Fig. 6(b) show typical fittings of NR and DPNR dielectric loss spectra at 283K. It is found that the fitting of NR spectra at 283K is satisfied by using a NM process and a conductivity term. For DPNR, this fitting is combined with a NM relaxation, a conductivity term and a new mode relaxation at lower frequency. Without resolving this new mode relaxation, the fitting is unacceptable mathematically. In fact, this new mode relaxation for DPNR can also be found in Fig. 3 as the dark yellow arrow indicates. Some of NM and this new mode relaxation fitting parameters in the illustrated spectra are also summarized in Table S2.

In order to compare the different NM relaxation quantitatively, VFT curves of NM and the new mode relaxation process for NR and DPNR are plotted in Fig. 7 as function of inverse temperature.

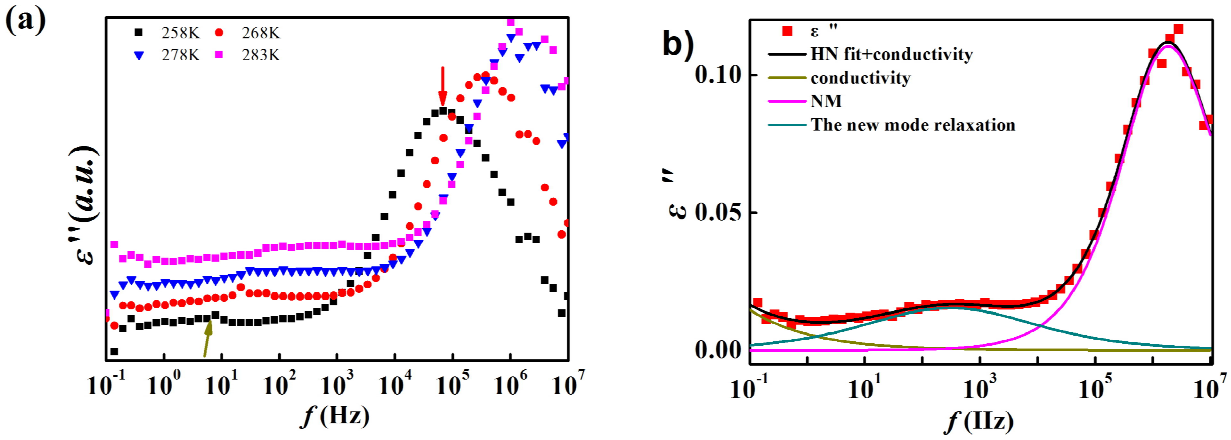

Fig.6 (a) Dielectric loss ε″ vs. frequency of DPNR at 258 to 283K indicates the emerging of the new mode relaxation peaks (as the dark yellow arrow) as well as the NM mode relaxation (as the red arrow). The curves at 268K, 278K and 283K are shifted vertically for clarity.

(b)Dielectric loss spectra of DPNR using a HN function for fitting at 283K

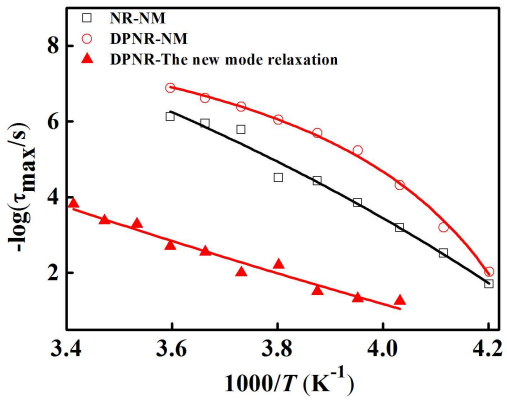

Fig.7 Activation plot for the normal relaxation for NR, DPNR and the new mode relaxation for DPNR. The lines represent the fits of Equation 6.

It demonstrates that τ_{max} of NM for DPNR is smaller than that for NR at the same temperature as shown in Table S2 and Fig. 7, which implies that DPNR without ω-terminal network exhibits faster dynamics than NR. Logically, this is expected because the mobility of NR long chain arms of the DPNR becomes much higher due to the absence of restriction from ω-terminals.

Here, in order to compare the different relaxation modes more distinctly for DPNR, VFT curves of SM, NM and the new mode for DPNR are specially plotted as function of inverse temperature in Fig. S6. Here, we can find that at the same temperature, the relaxation for NM is slower in about 2 orders of magnitude than that for SM. Moreover, the relaxation for the disclosed new mode is slower in 3~4 orders of magnitude comparing to NM. For instance, when T is 243K (1000/T of 4.115K^{-1}), the τ_{max} values for SM, NM and the new mode are 2.46×10^{-6} s, 6.25×10^{-4} s and 4.70×10^{-1} s, respectively. Since this new mode relaxation process moves to high frequency as the temperature increases (as the dark yellow arrow in Fig. 6(a)), it could be reasonably attributed to the relaxation of larger chain units and it is speculated that this new mode comes from the movement of phospholipids core of DPNR and can be named as branch mode (BM) relaxation. As for NR, phospholipids almost cannot move integrally because of the networking structure confinement. After deproteinization, the structure of natural rubber is converted from networking structure to branched structure with the phospholipids aggregates as the core and NR long chain as the arms. Without the fixation of ω-ends, the whole chain movement of DPNR becomes easier and activates the phospholipids core to move together. At the same time, due to the existence of chain constraints, the phospholipids core would not be free to explore the whole space and BM relaxation of the phospholipids core is slower than NM relaxation of NR long chain arms. As the disclosed new mode behaves as thermally activated process and it is significantly slower than normal mode for DPNR, it is rational to ascribe it as the branch mode for DPNR.

In order to confirm this speculation, it is necessary to further analyze the dielectric spectra of TE-DPNR. Fig. 3 shows that there is no dielectric loss peak at the temperature range of 248K to 273K for TE-DPNR, during which temperature BM relaxation emerges for DPNR. That is, when phospholipids are decomposed, this relaxation disappears. This fact further confirms that the new mode relaxation for DPNR is attributed to phospholipids core movement.

Fig. S7 shows dielectric loss vs. frequency of TE-DPNR. Since the intensity of NM dielectric loss for TE-DPNR is so weak (no more than 0.012) that it is difficult to carry out the HN fitting, the fitting for NM relaxation of TE-DPNR will not be provided in the present work. However, we can still find its NM characteristics from its temperature and frequency spectra. Fig. 3 shows that NM relaxation can be detectable at 268K, 228K and 308K for NR, DPNR and TE-DPNR, respectively (as the red arrows). It means that TE-DPNR has significantly slower NM relaxation than the other two systems. It seems to be contradictory since TE-DPNR possesses the lowest crosslinking density and the largest movement volume and it has been reported that the NM of the polymer stars is shown to be significantly slower than that of the corresponding arms.[47] Therefore, TE-DPNR is expected to

experience NM movement at the lowest temperature. However, Floudas *et al*. utilized dielectric spectroscopy to study selectively the SM and NM dynamics of PI where PI and polystyrene form the core and corona respectively and got the result that NM processes in *cis*-PI star models was faster than that in the linear PI with similar length as the arm chains of the star models when $M \approx 3M_e$, where M was the arm molecular weight and M_e was the molecular weight among entanglements.[50] The explanation has been given by the calculations based on the Rouse model. According to Floudas *et al.*,[50] the ratio of the NM relaxation time for star polymer, τ_{star} and that of the linear homogeneous polymer with similar length as the arm, τ_{linear} follows Equation 7 with the proportionality constant is the number of star arms.[50]

$$\frac{\tau_{star}}{\tau_{linear}} \propto \left(\frac{M_e}{M}\right)^3 \quad (7)$$

This relation predicts that the NM relaxation for star polymers will speed up if $M > 1.5M_e$ since the number of arms of phospholipids aggregates is almost 3 to 4. Considering the report that M_e for natural PI$\approx 3\cdot10^3$ and M of linear NR long chain $\approx 10^6$,[51] it is reasonable that DPNR has significantly faster NM relaxation than TE-DPNR, as experimentally observed here.

Besides SM and NM relaxations, TE-DPNR exhibits another relaxation at the temperature much lower than that of SM (as the blue arrow shown in Fig. 3) which is called as LTM (low temperature mode). This relaxation cannot be found either in NR or DPNR. Fig. 8(a) shows the dielectric loss of TE-DPNR as the function of the frequency at the temperature range of 173K to198K. From this figure, one can observe that the relaxation peak moves to high frequency with increasing temperature. The intensity of low temperature dielectric loss is between 0.015 and 0.02 at the temperature range of 173 to 198K, which is lower than SM relaxation (as shown in Fig. 4(c)). Typical fitting of the dielectric loss data using the HN function containing a conductivity term is shown in Fig. 8(b) at T=173K. As one can see, the fitting of the TE-DPNR spectra at 173K is performed using one HN relaxation process plus a conductivity term. Some of the fitting parameters of the LTM relaxation in the illustrated spectra are also presented in Table S2. Since this low temperature relaxation does not exist either in NR or DPNR, we infer that it comes from the movement of the mono- or di-phosphate groups which are associated with phospholipids by H-bonding or ionic bonds at the α- terminal in DPNR and NR. Before transesterification, these phosphate groups are linked with phospholipids further to contribute to the α-end networking. Therefore the movements are not possible. After transesterification, TE-DPNR has free mono- or di-phosphate groups at the α-terminal, which can have response to the dielectric environment. Therefore this new low temperature relaxation emerges.

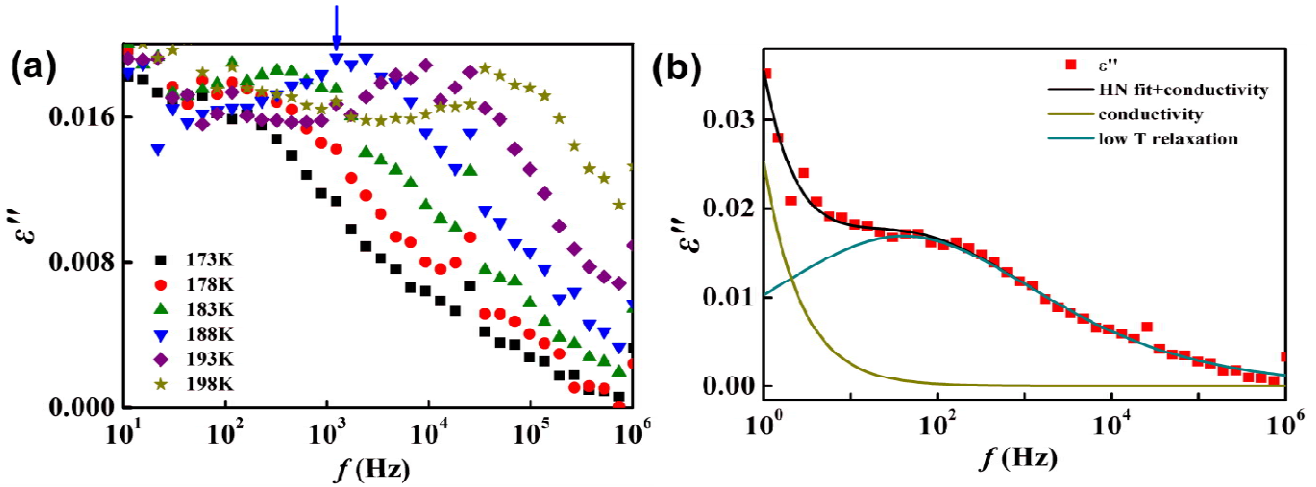

Fig.8 (a) Dielectric loss ε″ vs. frequency of TE-DPNR at 173K to 198K. The blue arrow indicates the peak of low temperature relaxation for TE-DPNR at 188K; (b) Dielectric loss spectra of TE-DPNR using a HN function for fitting at 173K.

Based on this observation above, a schematic model of dielectric relaxation for these progressively evolved samples is shown in Fig. 9. As a network structure, NR experiences a segmental relaxation at low temperature as well as a normal mode relaxation at high temperature. DPNR has branched structure and a faster normal relaxation compared to NR. At the same time, BM relaxation for DPNR appears at higher temperature compared to SM and NM relaxation and it is attributed to the movement of phospholipids core of DPNR. Transesterification of DPNR decomposes the phospholipids and makes TE-DPNR a linear structure similar to PI. Therefore, BM relaxation for DPNR disappears in TE-DPNR. At the same time, in TE-DPNR, there is a new mode relaxation at lower temperature than that for SM relaxation of TE-DPNR which cannot be found in NR and DPNR. This new low temperature relaxation may be ascribed to the free mono- or di-phosphate groups at α- terminal of TE-DPNR.

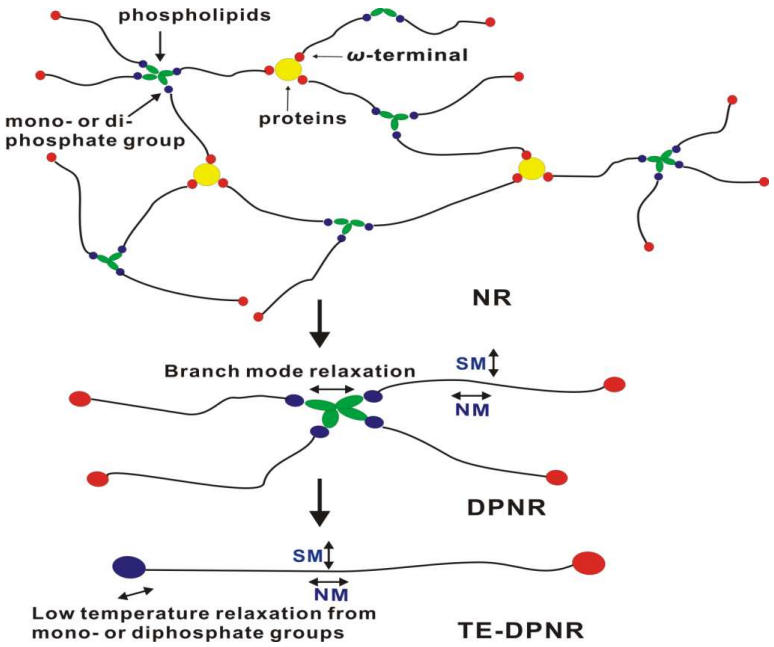

Fig.9 Schematic models of dielectric relaxation for NR, DPNR and TE-DPNR

Conclusions

In the present study, we performed detailed dielectric relaxation analysis to reveal the effects of proteins and phospholipids on the chain dynamics of natural rubber, together with the rheological measurements.

Distinctly different from the widely accepted segmental mode (SM) and normal mode (NM), a new relaxation mode in deproteinized NR (DPNR) is identified for the first time, which can't be found either in NR or in transesterified DPNR (TE-DPNR). Since this new mode relaxation process behaves as a thermally activated process and it is about 3~4 orders of magnitude slower than NM, it could be rationally attributed to the relaxation of the phospholipids core of DPNR, named as branch mode (BM) relaxation. When further conversion of DPNR into TE-DPNR is conducted, the phospholipids are removed and BM disappears. In addition, a new relaxation mode which occurs at much lower temperature than that for SM is revealed in TE-DPNR and it may be correlated to the relaxation of free mono- or di-phosphate groups at the α ends in TE-DPNR.

Deproteinization leads to slower SM relaxation while further transesterification speeds up the SM process to exceed that for NR. DPNR exhibits faster NM relaxation comparing to NR. However, NM relaxation of TE-DPNR is essentially slowed down compared with DPNR and NR.

The identification of the new relaxation modes in DPNR and TE-DPNR provide new evidence for the natural networking structure linked by protein-based ω ends and phospholipids-based α ends. The in-depth understanding on the natural networking is significant as it provides insights for mimicking NR natural networking with synthesized polyisoprene, which has profound significance to solve the shortage of NR.

Acknowledgements

This work was supported by National Natural Science Foundation of China (51222301 and 51333003) and Fundamental Research Project for the Central Universities (2014ZG0001).

Notes and references

[a] *Department of Polymer Materials and Engineering, South China University of Technology, Guangzhou 510640, China. E-mail: psbcguo@scut.edu.cn; Fax: +86 20 22236688; Tel: +86 20 87113374*

[b] *College of Polymer Science and Engineering, State Key Laboratory of Polymer Materials Engineering, Sichuan University, Chengdu, 610065, China. E-mail: guangsu-huang@hotmail.com*

† Electronic Supplementary Information (ESI) available: [Stress-strain curves of NR, DPNR and TE-DPNR]. See DOI: 10.1039/b000000x/

1 Y. Tanaka, *Rubber Chem. Technol.*, 2001, **74**, 355-375.
2 S. Amnuaypornsri, J. Sakdapipanich and Y. Tanaka, *J. Appl. Polym. Sci.*, 2009, **111**, 2127-2133.
3 J. Tangpakdee and Y. Tanaka, *Rubber Chem. Technol.*, 1997, **70**, 707-713.
4 J. Carretero-Gonzalez, T. A. Ezquerra, S. Amnuaypornsri, S. Toki, R. Verdejo, A. Sanz, J. Sakdapipanich, B. S. Hsiao and M. A. Lopez-Manchado, *Soft Matter*, 2010, **6**, 3636-3642.
5 L. Tarachiwin, J. Sakdapipanich, K. Ute, T. Kitayama, T. Bamba, E. Fukusaki, A. Kobayashi and Y. Tanaka, *Biomacromolecules*, 2005, **6**, 1851-1857.
6 D. Boese and F. Kremer, *Macromolecules*, 1990, **23**, 829-835.
7 J. Mijovic, H. K. Lee, J. Kenny and J. Mays, *Macromolecules*, 2006, **39**, 2172-2182.
8 S. Toki, C. Burger, B. S. Hsiao, S. Amnuaypornsri, J. Sakdapipanich and Y. Tanaka, *J. Polym. Sci. Pol. Phys.*, 2008, **46**, 2456-2464.
9 O. Chaikumpollert, Y. Yamamoto, K. Suchiva, P. T. Nghia and S. Kawahara, *Polym. Advan. Technol.*, 2012, **23**, 825-828.
10 L. Tarachiwin, J. Sakdapipanich, K. Ute, T. Kitayama and Y. Tanaka, *Biomacromolecules*, 2005, **6**, 1858-1863.
11 S. Kawahara, K. Takano, J. Yunyongwattanakorn, Y. Isono, M. Hikosaka, J. T. Sakdapipanich and Y. Tanaka, *Polym. J.*, 2004, **36**, 361-367.

12 S. Amnuaypornsri, A. Nimpaiboon and J. Sakdapipanich, *Kaut. Gummi. Kunst.*, 2009, **62**, 88-92.
13 S. Amnuaypornsri, S. Toki, B. S. Hsiao and J. Sakdapipanich, *Polymer*, 2012, **53**, 3325-3330.
14 S. Kawahara, Y. Inomata, T. Kakubo, Y. Tanaka, K. Hatada, K. Ute and N. Miyatake, *Rubber Chem. Technol.*, 1998, **71**, 277-284.
15 J. Yunyongwattanakorn, J. T. Sakdapipanich, S. Kawahara, M. Hikosaka and Y. Tanaka, *J. Appl. Polym. Sci.*, 2007, **106**, 455-461.
16 S. Amnuaypornsri, J. Sakdapipanich, S. Toki, B. S. Hsiao, N. Ichikawa and Y. Tanaka, *Rubber Chem. Technol.*, 2008, **81**, 753-766.
17 S. Toki, B. S. Hsiao, S. Amnuaypornsri and J. Sakdapipanich, *Polymer*, 2009, **50**, 2142-2148.
18 S. Amnuaypornsri, S. Kawahara, S. Toki, B. S. Hsiao, M. Hikosaka, J. Sakdapipanich and Y. Tanaka, *Kaut. Gummi. Kunst*, 2012, **65**, 46-50.
19 K. Nawamawat, J. T. Sakdapipanich, C. C. Ho, Y. J. Ma, J. Song and J. G. Vancso, *Colloid Surface A*, 2011, **390**, 157-166.
20 S. Toki, J. Che, L. X. Rong, B. S. Hsiao, S. Amnuaypornsri, A. Nimpaiboon and J. Sakdapipanich, *Macromolecules*, 2013, **46**, 5238-5248.
21 K. Suchiva, T. Kowitteerawut and L. Srichantamit, *J. Appl. Polym. Sci.*, 2000, **78**, 1495-1504.
22 S. Amnuaypornsri, J. Sakdapipanich and Y. Tanaka, *J. Appl. Polym. Sci.*, 2010, **118**, 3524-3531.
23 N. Rattanasom and O. Chaikumpollert, *J. Appl. Polym. Sci.*, 2003, **90**, 1793-1796.
24 S. S. Sarkawi, W. K. Dierkes and J. W. M. Noordermeer, *Eur. Polym. J.*, 2013, **49**, 3199-3209.
25 H. H. Le, S. Abhijeet, S. Ilisch, J. Klehm, S. Henning, M. Beiner, S. S. Sarkawi, W.Dierkesg, A. Das, D. Fischer, K.-W. Stockelhuber, S. Wiessner, S. P. Khatiwada, R. Adhikari, T. Pham, G. Heinrich and H.-J. Radusch, *Polymer*, 2014, **55**, 4738-4747.
26 H. H. Le, M. Parsekar, S. Ilisch, S. Henning, A. Das, K. -W. Stockelhuber, M. Beiner, C. A. Ho, R. Adhikari, S. Wiener, G. Heinrich and H. –J. Radusch, *Macromol. Mater. Eng.*, 2014, **299**, 569-582.
27 S. S. Sarkawi, W. K. Dierkes and J. W. M. Noordermeer, *Kaut. Gummi. Kunst.*, 2013, **66**, 27-33.
28 K. Nor-Hidayaty, K. Shamsul, M. Asrul and K. Ahmad-Nazir, *J. Rubber Res.*, 2011, **14**, 129-138.
29 N. Rattanasom, U. Thammasiripong and K. Suchiva, *J. Appl. Polym. Sci.*, 2005, **97**, 1139-1144.
30 P. G. Santangelo and C. M. Roland, *Rubber Chem. Technol.*, 2003, **76**, 892-898.
31 K. Nawamawat, J. T. Sakdapipanich and C. C. Ho, *Macromol. Symp.*, 2010, **288**, 95-103.
32 S. Cerveny, P. Zinck, M. Terrier, S. Arrese-Igor, A. Alegria and J. Colmenero, *Macromolecules*, 2008, **41**, 8669-8676.
33 M. Hernandez, M. A. Lopez-Manchado, A. Sanz, A. Nogales and T. A. Ezquerra, *Macromolecules*, 2011, **44**, 6574-6580.
34 D. Boese, F. Kremer, L. J. Fetters, *Macromolecules*, 1990, **23**, 1826-1830
35 K. A. Page and K. Adachi, *Polymer*, 2006, **47**, 6406-6413.
36 A. Arbe, A. Alegria, J. Colmenero, S. Hoffmann, L. Willner and D. Richter, *Macromolecules*, 1999, **32**, 7572-7581.
37 P. G. Santangelo and C. M. Roland, *Macromolecules*, 1998, **31**, 3715-3719.
38 M. Hernandez, J. Carretero-Gonzalez, R. Verdejo, T. A. Ezquerra and M. A. Lopez-Manchado, *Macromolecules*, 2010, **43**, 643-651.
39 P. Ortiz-Serna, R. Diaz-Calleja, M. J. Sanchis, E. Riande, R. Nunes, A. Martins and L. Visconte, *J. Non-Crystal. Solids*, 2011, **357**, 598-604.
40 P. Ortiz-Serna, R. Diaz-Calleja, M. J. Sanchis, G. Floudas, R. C. Nunes, A. F. Martins and L. L. Visconte, *Macromolecules*, 2010, **43**, 5094-5102.
41 D. Fragiadakis, L. Bokobza, P. Pissis, *Polymer*, 2011, **52**, 3175-3182.
42 W. Pichayakorn, J. Suksaeree, P. Boonme, W. Taweepreda and G. C. Ritthidej, *Ind. Eng. Chem. Res.*, 2012, **51**, 13393-13404.
43 J. T. Sakdapipanich, T. Kowitteerawut, K. Suchiva and Y. Tanaka, *Rubber Chem. Technol.*, 1999, **72**, 712-720.
44 S. Kawahara, T. Kakubo, N. Nishiyama, Y. Tanaka, Y. Isono and J. T. Sakdapipanich, *J. Appl. Polym. Sci.*, 2000, **78**, 1510-1516.
45 T. Karino, Y. Ikeda, Y. Yasuda, S. Kohjiya and M. Shibayama, *Biomacromolecules*, 2007, **8**, 693-699.
46 S. W. Wu, Z. H. Tang, B. C. Guo, L. Q. Zhang and D. M. Jia, *RSC Adv.*, 2013, **3**, 14549-14559.
47 W. W. Graessley, *Adv. Polym. Sci.*, 1982, **47**, 67-117.
48 R. Diaz-Calleja, *Macromolecules*, 2000, **33**, 8924-8924.
49 V. Y. Kramarenko, T. A. Ezquerra, I. Sics, F. J. Balta-Calleja and V. P. Privalko, *J. Chem. Phys.*, 2000, **113**, 447-452.
50 G. Floudas, S. Paraskeva, N. Hadjichristidis, G. Fytas, B. Chu and A. N. Semenov, *J. Chem. Phys.*, 1997, **107**, 5502-5509.
51 L. J. Fetters, D. J. Lohse, D. Richter, T. A. Witten, A. Zirkel, *Macromolecules*, 1994, **27**, 4639-4647.